Food and Chemical Toxicology 62 (2013) 638–644

Contents lists available at ScienceDirect

Food and Chemical Toxicology

journal homepage: www.elsevier.com/locate/foodchemtox

Anti-inflammatory effect of austroinulin and 6-O-acetyl-austroinulin from *Stevia rebaudiana* in lipopolysaccharide-stimulated RAW264.7 macrophages

Byoung Ok Cho [a], Hyung Won Ryu [a,1], Yangkang So [a], Jung Keun Cho [a], Hyun Sim Woo [a], Chang Hyun Jin [a], Kwon Il Seo [b], Jong Chun Park [c], Il Yun Jeong [a,*]

[a] Advanced Radiation Technology Institute, Korea Atomic Energy Research Institute, Jeongeup, Jeonbuk 580-185, Republic of Korea
[b] Department of Food and Nutrition, Sunchon National University, Sunchon, Jeonnam 540-742, Republic of Korea
[c] Department of Microbiology, College of Medicine, Seonam University, Namwon, Jeonbuk 590-711, Republic of Korea

ARTICLE INFO

Article history:
Received 20 March 2013
Accepted 7 September 2013
Available online 17 September 2013

Keywords:
Austroinulin
6-O-acetyl-austroinulin
NO
Pro-inflammatory cytokine
STAT1
IRF3

ABSTRACT

Austroinulin (AI) and 6-O-acetyl-austroinulin (6-OAAI) are natural diterpenoids isolated from *Stevia rebaudiana* with anti-inflammatory activity. However, the mechanisms underlying their anti-inflammatory effects are not well understood. The purpose of this study was to investigate the effect of AI and 6-OAAI on nitric oxide (NO) production and their molecular mechanism in LPS-stimulated RAW264.7 macrophages. We found that AI and 6-OAAI inhibit the production of NO, iNOS, and pro-inflammatory cytokines (TNF-α, IL-6, IL-1β, and MCP-1) in LPS-stimulated RAW264.7 macrophages. In these same cells, AI and 6-OAAI also suppressed the phosphorylation of STAT1 and the production of interferon-beta (IFN-β). Moreover, treatment with AI and 6-OAAI inhibited the activation of interferon regulatory factor-3 (IRF3) and NF-κB. Taken together, our results suggest that AI and 6-OAAI inhibit NO production and iNOS expression by blocking the activation of STAT1, IRF3, and NF-κB in LPS-stimulated RAW264.7 macrophages.

1. Introduction

Inflammation is part of the non-specific immune response that occurs in reaction to any type of bodily injury. The innate immune system is the first response to infection and plays a critical role in acute inflammation. The infiltration of neutrophils and macrophages characterizes acute inflammation, while the infiltration of T lymphocytes and plasma cells are features of chronic inflammation (Ferrero-Miliani et al., 2006). Chronic and uncontrolled inflammation may cause the pathogenesis of a variety of diseases, such as arthritis, asthma, multiple sclerosis, inflammatory bowel disease, and atherosclerosis (Kim et al., 2010). Macrophages play a central role in inflammatory diseases and produce many pro-inflammatory cytokines, such as interleukin-6 (IL-6), tumor necrosis factor-α (TNF-α), and interleukin-1β (IL-1β). Macrophages also produce inflammatory mediators, including nitric oxide (NO) and prostaglandin E_2 (PGE_2) (Heo et al., 2010). As the major component of the outer membrane of Gram negative bacteria cell walls, lipopolysaccharide (LPS) can stimulate macrophages to produce pro-inflammatory cytokines, including TNF-α and IL-6, and inflammatory mediators such as NO and PGE_2 (Lu et al., 2012). NO is produced by inducible nitric oxide synthase (iNOS) and mediates many disease processes, such as atherosclerosis, inflammation, carcinogenesis, hypertension, obesity, and diabetes (Mordan et al., 1993; Ohshima and Bartsch, 1994; KrÖche et al., 1998). Therefore, inhibition of these pro-inflammatory mediators may be an effective strategy for the treatment of inflammatory diseases.

Stevia rebaudiana Bertoni is a branched bushy shrub that belongs to the Asteraceae family and is native to Paraguay, Brazil, and Argentina. Today, it is also cultivated in Canada and in some parts of Asia and Europe (Lemus-Mondaca et al., 2012). Extracts from *Stevia* leaves have been used in traditional medicine for the treatment of diabetes. It is also used to sweeten soft drinks, soju, soy sauce, yogurt, and other foods in Japan, Korea, and certain countries of South America (Shukla et al., 2009). Several studies have demonstrated that *S. rebaudiana* sweetener extractives possess anti-hypertensive, anti-hyperglycemic, and anti-human rotavirus activities (Chan et al., 2000; Jeppesen et al., 2002; Lee and Shibamoto, 2001). A recent study has reported that the essential oil and extracts from *S. rebaudiana* leaves exhibit antioxidant,

* Corresponding author. Address: Advanced Radiation Technology Institute, Korea Atomic Energy Research Institute, 1266 Sinjeong, Jeongeup, Jeonbuk 580-185, Republic of Korea. Tel.: +82 63 570 3150; fax: +82 63 570 3159.
E-mail address: iyjeong@kaeri.re.kr (I.Y. Jeong).
[1] Present address: Natural Medicine Research Center, Korea Research Institute of Bioscience and Biotechnology, Ochang-eup, Cheongwon-gun, Chungbuk 363-883, Republic of Korea.

0278-6915/$ - see front matter © 2013 Elsevier Ltd. All rights reserved.
http://dx.doi.org/10.1016/j.fct.2013.09.011

anti-microbial, and anti-inflammatory effects (Muanda et al., 2011). The leaves of *Stevia* contain flavonoids, alkaloids chlorophylls, xanthophylls, hydroxycynnamic acids, oligosaccharides, free sugars, amino acids, lipids, and trace elements (Muanda et al., 2011). In addition, the leaves of *Stevia* are known to contain diterpenoid glycosides, including stevioside, steviolbioside, rebaudioside A–F, and dulcoside, as well as diterpenes, such as sterebin A-N and 6-O-acetyl-austroinulin (Oshima et al., 1986, 1988; Dacome et al., 2005). It has been reported that diterpene contents exhibit antioxidant, anti-bacterial, and anti-viral activity (Wang et al., 2002; Porto et al., 2009; Vallim et al., 2010). However, the biological activities of these components have not yet been fully defined. Therefore, the aim of the present study was to characterize austroinulin (AI) and 6-O-acetyl-austroinulin (6-OAAI) isolated from *S. rebaudiana* based on the results of NMR and other analytical data and to evaluate their anti-inflammatory effects in LPS-stimulated RAW264.7 macrophages.

2. Materials and methods

2.1. Materials

The leaves of *S. rebaudiana* used in the present study, which were collected in the Jeonbuk province in Korea, were purchased from Koreastevia Co., Ltd. (http://www.koreastevia.com/, Jeongeup, Korea) in October 2010. The leaves were air-dried, pulverized, and stored at 4 °C before extraction. All chemicals used were of reagent grade and were purchased from Sigma–Aldrich (St. Louis, MO, USA), unless otherwise stated. All solvents were distilled before use. Antibodies for β-Tubulin and iNOS were purchased from Santa Cruz Biotechnology (Santa Cruz, CA, USA) and BD Pharmingen (San Diego, CA, USA), respectively. Antibodies for STAT1 and phospho-STAT1 (Tyr701) were purchased from Cell Signaling Technology (Danvers, MA, USA). Goat anti-rabbit IgG HRP-conjugated antibody, Opti-MEM I medium, and Lipofectamine 2000 were purchased from Invitrogen (Carlsbad, CA, USA). Enzyme-linked immunosorbent assay (ELISA) kits for IFN-β, MCP-1, TNF-α, IL-6, and IL-1β were purchased from R&D Systems (Minneapolis, MN, USA).

2.2. General procedure

NMR spectra were recorded on a JEOL ECX-500 instrument (^{1}H NMR at 500 MHz, ^{13}C NMR at 125 MHz) (JEOL, Tokyo, Japan). Electron ionization (EI) and EI-high resolution (HR) mass spectra were obtained on a JEOL JMS-700 instrument (JEOL Ltd., Tokyo, Japan). Melting points were measured on a Thomas Scientific Capillary Melting Point Apparatus and were uncorrected. Column chromatography was performed on silica gel (230–400 mesh; Merck, Darmstadt, Germany), RP-18 (ODS-A, 12 nm, S-150 μM; YMC, Kyoto, Japan) and Sephadex LH-20 (GE Healthcare Bio-Science AB, Björkgatan, Sweden). Thin layer chromatography (TLC) was performed on precoated TLC plates on silica gel 60 F254 (0.25 mm, normal phase; Merck). These were visualized using a UVGL-58 254 nm hand-held UV lamp (UVP, Cambridge, UK) or by spraying with 10% H_2SO_4 in ethanol followed by heating. Acetone-d6 and DMSO-d6 were purchased from Cambridge Isotope Laboratory Inc. (Andover, MA, USA).

2.3. Extraction and isolation of compounds from S. rebaudiana

The dried leaves of *S. rebaudiana* (1 kg) were extracted three times with 80% ethanol, and the supernatant was evaporated under vacuum at 40 °C. The ethanol extract was dissolved in distilled water and partitioned with ethyl acetate. Evaporation of the solvent under reduced pressure yielded the ethyl acetate extract (50 g), which was fractionated on a silica gel column (10 × 30 cm, 230–400 mesh, 700 g) and eluted using hexane/acetone [50:1 (1.5 L), 40:1 (1.5 L), 20:1 (1.5 L), 10:1 (3 L), 8:1 (2.5 L), 6:1 (2 L), 3:1 (2 L), 1:1 (1 L), and then only acetone (2 L)] to give eight pooled fractions F1–F7 based on comparison of TLC profiles. Subfraction F5 was subjected to flash column chromatography (2.5 × 30 cm, 230–400 mesh, 200 g) employing a hexane/ethyl acetate gradient (20:1 → 1:1) to give compound **1** (385 mg) and **2** (185 mg) (Fig. 1). Finally, the purified compound was identified by comparing its ^{1}H and ^{13}C NMR data with published literature (Supplementary materials) (Quijano et al., 1982; Sholichin et al., 1980).

2.4. Austroinulin (*1*)

White crystals; mp 75–78 °C; $[\alpha]_D$ + 33.6° ($CHCl_3$, *c* 0.48); EIMS: *m/z* $[M]^+$ 322; HREIMS *m/z* 322.2508 (calcd for $C_{20}H_{34}O_3$, 322.2508); ^{1}H NMR (500 MHz, $CDCl_3$) δ 0.87 (3H, s, H-18), 0.96 (3H, s, H-20), 1.11 (3H, s, H-17), 1.14 (3H, s, H-19), 1.11–1.51 (6H, m, H-1,2,3,5,9), 1.76 (3H, s, H-16), 2.21 (1H, m, H-11a), 2.40 (1H, m, H-11b), 3.39 (1H, t, *J* = 10 Hz, H-7), 3.58 (1H, t, *J* = 10 Hz, H-6), 5.08, 5.17(2H, br d, *J* = 17 Hz, H-15), 5.43(1H, t, *J* = 6.6 Hz, H-12), 6.83(1H, d, *J* = 17 Hz, H-14); ^{13}C NMR (500 MHz, CDCl3) δ 17.0 (C-20), 18.2 (C-2), 19.4 (C-17), 19.9 (C-16), 22.3 (C-19), 22.8 (C-11), 33.8 (C-4), 36.4 (C-18), 39.2 (C-10), 39.9 (C-10), 43.4 (C-3), 57.3 (C-5), 59.6 (C-9), 71.7 (C-6), 77.3 (C-8), 85.0 (C-7), 113.8 (C-15), 130.9 (C-13), 133.6 (C-12), 133.7 (C-14).

2.5. 6-O-acetyl-austroinulin (*2*)

White crystals; mp 174–175 °C; $[\alpha]_D$ + 36.8° ($CHCl_3$, *c* 0.46); EIMS: *m/z* $[M]^+$ 364; HREIMS *m/z* 364.2614 (calcd for $C_{22}H_{36}O_4$, 322.2614); ^{1}H NMR (500 MHz, $CDCl_3$) δ 0.84 (3H, s, H-18), 0.92 (3H, s, H-20), 0.97 (3H, s, H-19), 1.18 (3H, s, H-17), 1.18–1.51 (6H, m, H-1,2,3,5,9), 1.75 (3H, s, H-16), 2.08 (3H, s, H-22), 2.21 (1H, m, H-11a), 2.42 (1H, m, H-11b), 3.43 (1H, t, *J* = 10 Hz, H-7), 3.45 (1H, t, *J* = 10 Hz, H-6), 5.07, 5.17(2H, br d, *J* = 17 Hz, H-15), 5.42(1H, t, *J* = 6.6 Hz, H-12), 6.82 (1H, d, *J* = 17 Hz, H-14); ^{13}C NMR (500 MHz, CDCl3) δ 16.8 (C-20), 18.1 (C-2), 19.5 (C-17), 19.9 (C-16), 21.9 (C-22), 22.2 (C-19), 22.8 (C-11), 33.4 (C-4), 36.0 (C-18), 39.4 (C-10), 39.8 (C-10), 43.5 (C-3), 56.5 (C-5), 59.2 (C-9), 73.3 (C-6), 77.1 (C-8), 83.5 (C-7), 113.8 (C-15), 130.9 (C-13), 133.5 (C-14), 133.7 (C-12) 171.9 (C-20).

2.6. Cell culture

RAW264.7 macrophage cells were purchased from American Type Culture Collection (Manassas, VA, USA). The cells were cultured in DMEM supplemented with 10% fetal bovine serum (Hyclone, Logan, UT, USA), 100 units/mL of penicillin, and 100 μg/mL of streptomycin (Invitrogen, Carlsbad, CA, USA) and maintained in a humidified incubator at 37 °C with 5% CO_2.

2.7. Cytotoxicity assay

To measure cell viability, we used an EZ-Cytox cell viability assay kit (DAEIL lab, Seoul, Korea). RAW264.7 cells were cultured in a 96-well plate at a density of 2×10^5 cells/mL for 24 h. The cells were subsequently treated with various concentrations of AI or 6-OAAI (10, 20, 40, 60, 80, and 100 μM). After culturing for 24 h, 10 μL of the kit solution was added to each well and incubated for 4 h at 37 °C and 5% CO_2. The index of cell viability was determined by measuring formazan production with an ELISA reader (Benchmark Plus, Bio-Rad, Hercules, CA, USA) at an absorbance of 480 nm. The reference wavelength was 650 nm. Cell viability was determined relative to untreated control cells.

2.8. Measurement of NO production

RAW264.7 cells were cultured in a 96-well plate at a density of 2×10^5 cells/mL for 24 h. After incubation, the cells were pretreated with various concentrations of AI or 6-OAAI (10, 20, and 40 μM) for 1 h and were treated with 1 μg/mL of LPS (Sigma–Aldrich) for an additional 16 h. The culture supernatant was collected at the end of the culture period for a nitrite assay. The culture supernatant (100 μL) was mixed with an equal volume of Griess reagent (Sigma–Aldrich) in a 96-well plate. After 15 min incubation at room temperature, the absorbance was measured at 540 nm. The concentration of nitrite was calculated using a standard curve produced from known concentrations of sodium nitrite dissolved in DMEM. The results are presented as the mean ± SD of four replicates of one representative experiment.

2.9. Western blotting

RAW264.7 cells were cultured in a 100 mm dish at a density of 2×10^5 cells/mL for 24 h. After incubation, the cells were pretreated with various concentrations of AI or 6-OAAI (10, 20, and 40 μM) for 1 h and were treated with 1 μg/mL of LPS for the indicated times. The cells were harvested and lysed by cell lysis buffer (50 mM Tris, pH 7.4, 250 mM NaCl, 5 mM EDTA, 50 mM NaF, 1 mM Na_3VO_4, 1% NP40, 0.02% NaN_3, and 1 mM PMSF) containing a protease inhibitor cocktail (Sigma–Aldrich) for 30 min on ice, and the cell extracts were then centrifuged. After quantification of protein concentration, equal amounts of protein were separated in SDS–polyacrylamide gels and transferred onto nitrocellulose membranes (Hybond ECL Nitrocellulose; Amersham Biosciences, Bucks, UK). The membranes were then blocked with

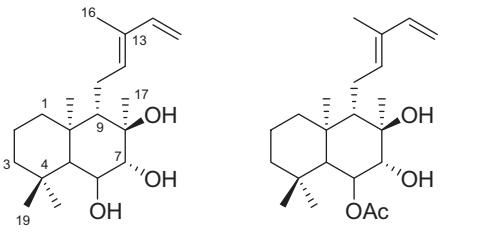

Austroinulin (**1**) 6-O-Acetyl-austroinulin (**2**)

Fig. 1. Chemical structure of compound **1** and **2**.

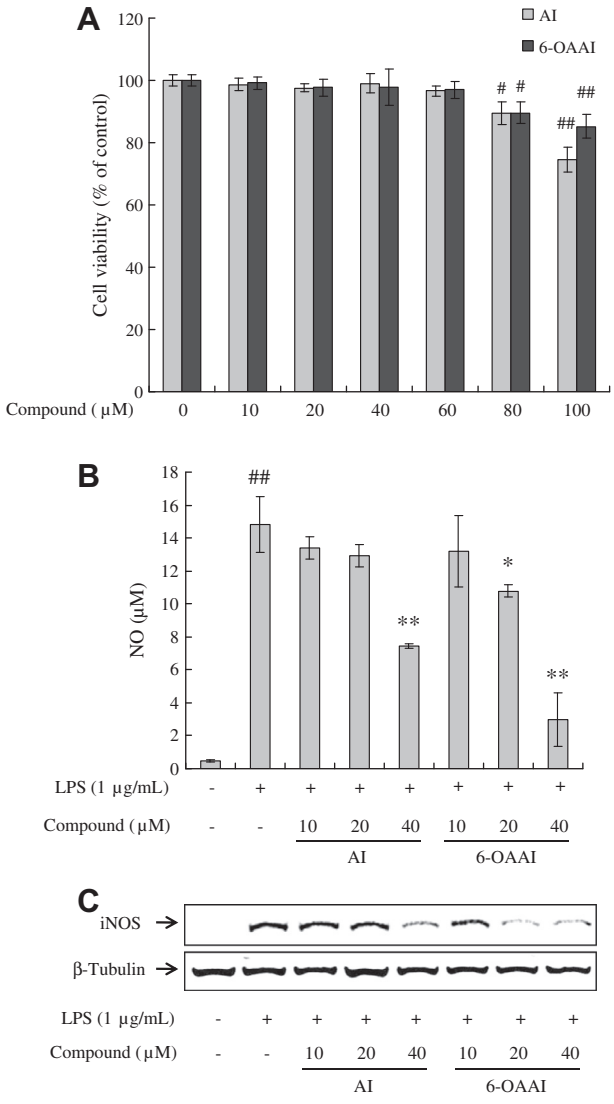

Fig. 2. Effect of AI and 6-OAAI on cell viability (A), NO production (B), and iNOS expression levels (C) in LPS-stimulated RAW264.7 macrophages. (A) RAW264.7 cells were treated with various concentrations of AI and 6-OAAI (10, 20, 40, 60, 80, and 100 μM) for 24 h, and the relative cell viability was assessed by WST-1 assay. (B) RAW264.7 cells were treated with various concentrations of AI and 6-OAAI (10, 20, and 40 μM) for 1 h prior to the addition of LPS (1 μg/mL), and the cells were further incubated for 16 h. The culture supernatant was subjected to a nitrite assay. Error bars represent the mean ± SD. $^{\#}p < 0.01$ vs. control, $^{\#\#}p < 0.001$ vs. control, $^{*}p < 0.05$ vs. LPS, $^{**}p < 0.01$ vs. LPS. (C) The iNOS expression levels were determined by western blotting.

5% nonfat dried milk in TBS-T (10 mM Tris–HCl pH 7.4, 150 mM NaCl, and 0.1% Tween 20) and incubated with the target antibodies overnight at 4 °C. After incubation, the membranes were washed, incubated with HRP conjugated secondary antibody for 2 h at room temperature, and then washed again. The protein bands were detected using an enhanced chemiluminescence detection system (GE Healthcare, Bucks, UK).

2.10. Measurement of IFN-β, MCP-1, TNF-α, IL-6, and IL-1β

The quantities of IFN-β, MCP-1, TNF-α, IL-6, and IL-1β in cell supernatant were measured using an ELISA kit (R&D Systems) according to the manufacturer's protocol. The results are presented as the mean ± SD of three replicates from one representative experiment.

2.11. Luciferase assay

RAW264.7 cells were cultured in a 6-well plate at a density of 4×10^5 cells/mL for 24 h. The pIRF3-luc reporter vector (kind gift from Dr. Katherine Fitzgerald, University of Massachusetts Medical School, Worcester, MA), the pNF-κB-luc reporter vector (Stratagene, La Jolla, CA, USA), and the pRL-TK internal control vector (Promega, Madison, WI, USA) were transfected with Lipofectamine 2000 (Invitrogen) according to the manufacturer's instructions. After transfection, the cells were pretreated with various concentrations of AI or 6-OAAI (10, 20, and 40 μM) for 1 h and were treated with 1 μg/mL of LPS for an additional 24 h. The cells were then collected. Luciferase activity was measured using the Dual-luciferase Reporter Assay System (Promega).

2.12. Statistical analysis

All data are presented as the mean ± SD. The significance of differences between the means of the treated and untreated groups was determined by Student's *t* test. A p value < 0.05 was considered to be significant.

3. Results

3.1. Effect of AI and 6-OAAI on cell cytotoxicity in RAW264.7 cells

RAW264.7 cells were treated with various concentrations of AI or 6-OAAI for 24 h, and cell viability was examined using the EZ-Cytox cell viability assay kit. As shown in Fig. 2A, AI and 6-OAAI did not exhibit cytotoxicity to RAW264.7 cells up to 60 μM but did inhibit cell viability at the doses of 80 and 100 μM. Based on these results, a dose of less than 40 μM of AI and 6-OAAI was used in subsequent experiments.

3.2. Effect of AI and 6-OAAI on NO production and iNOS protein expression levels in LPS-stimulated RAW264.7 cells

To evaluate whether AI and 6-OAAI possess potential anti-inflammatory effects in LPS-stimulated RAW264.7 cells, we investigated the inhibitory effects of AI and 6-OAAI on NO production (Fig. 2B). LPS treatment significantly increased the concentrations of NO when compared with the untreated cells ($p < 0.001$). However, the increase of NO production was significantly suppressed in the cells pretreated with AI or 6-OAAI in a dose-dependent manner. To further determine the cause of decreased NO production by AI and 6-OAAI, the expression of iNOS was measured by western blot. As expected, the expression of iNOS was significantly increased in the LPS-treated cells. However, LPS-induced expression of iNOS was reduced by pretreating cells with AI or 6-OAAI in a dose-dependent manner (Fig. 2B). These results strongly suggested that AI and 6-OAAI decreased NO production by suppression of iNOS expression. Furthermore, we found that 6-OAAI inhibited NO production and iNOS expression more effectively than AI.

3.3. Effect of AI and 6-OAAI on TNF-α, IL-6, IL-1β, and MCP-1 production in LPS-stimulated RAW264.7 cells

To determine the effects of AI and 6-OAAI on the production of the pro-inflammatory cytokines TNF-α, IL-6, IL-1β, and MCP-1, RAW264.7 cells were pretreated with various concentrations of AI or 6-OAAI (10, 20, and 40 μM) and stimulated with 1 μg/mL of LPS for 16 h. As shown in Fig. 3, the levels of TNF-α ($p < 0.001$), IL-6 ($p < 0.001$), IL-1β ($p < 0.01$), and MCP-1 ($p < 0.001$) were significantly increased in the LPS-treated cells when compared with the untreated cells. However, the levels of TNF-α, IL-6, IL-1β, and MCP-1 were significantly reduced in the cells pretreated with AI or 6-OAAI in a dose-dependent manner. These results also indicated that 6-OAAI inhibited the production of TNF-α, IL-6, IL-1β, and MCP-1 more effectively than AI.

3.4. Effect of AI and 6-OAAI on IFN-β production and STAT1 activation in LPS-stimulated RAW264.7 cells

To address the mechanism by which AI and 6-OAAI reduce LPS-induced NO production and iNOS expression, we analyzed the

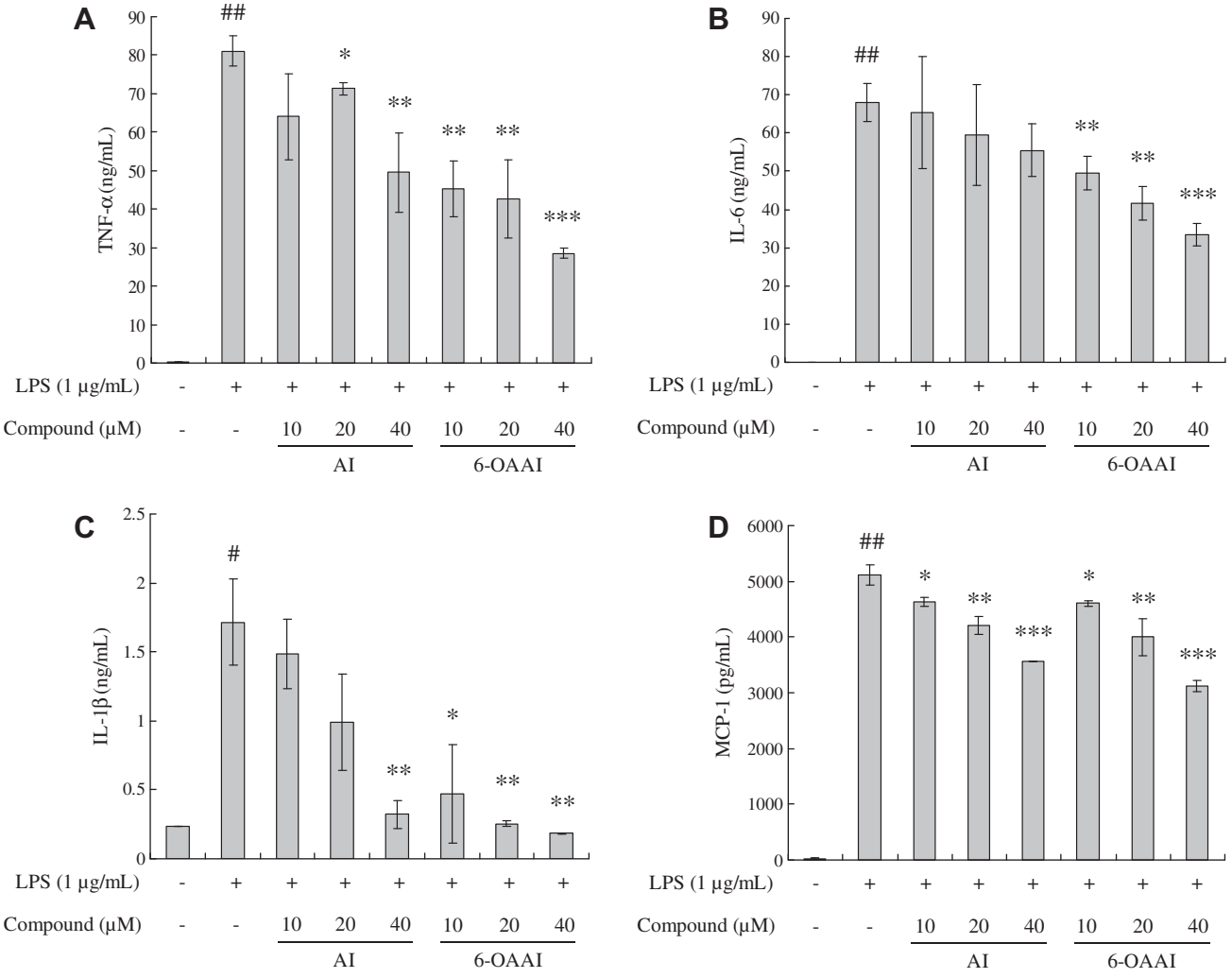

Fig. 3. Effect of AI and 6-OAAI on TNF-α (A), IL-6 (B), IL-1β (C), and MCP-1 (D) production in LPS-stimulated RAW264.7 macrophages. RAW264.7 cells were treated with various concentrations of AI and 6-OAAI (10, 20, and 40 μM) for 1 h prior to the addition of LPS (1 μg/mL), and the cells were further incubated for 16 h. The culture supernatant was subjected to ELISA. Error bars represent the mean ± SD. $^{\#\#}p < 0.001$ vs. control, $^{*}p < 0.05$ vs. LPS, $^{**}p < 0.01$ vs. LPS, $^{***}p < 0.001$ vs. LPS.

ability of AI and 6-OAAI to influence LPS-induced IFN-β production and STAT1 activation. As shown in Fig. 4A, the levels of IFN-β ($p < 0.001$) were significantly increased in the LPS-treated cells when compared with the untreated cells. However, the levels of IFN-β were significantly decreased in the cells pretreated with AI or 6-OAAI in a dose-dependent manner. Moreover, the phosphorylation of STAT1 increased in the LPS-treated cells as shown by western blot. However, AI or 6-OAAI treatment in the LPS-treated cells decreased the phosphorylation of STAT1 in a dose-dependent manner (Fig. 4B). We also found that 6-OAAI inhibited the production of IFN-β and the phosphorylation of STAT1 more effectively than AI.

3.5. Effect of AI and 6-OAAI on IRF3 and NF-κB activation in LPS-stimulated RAW264.7 cells

The above results demonstrate that AI and 6-OAAI inhibit LPS-induced production of IFN-β, pro-inflammatory cytokines, and iNOS. To further identify the mechanism by which AI and 6-OAAI exhibit anti-inflammatory effects in LPS-stimulated RAW264.7 cells, we assessed the activation of IRF3 and NF-κB by a reporter gene assay. RAW264.7 cells were transiently transfected with the pIRF3-luc plasmid (containing the IFN-β promoter domain with the IRF3 binding site) or the pNF-κB-luc plasmid (containing repeats of NF-κB recognition sequences). As shown in Fig. 5, LPS treatment significantly increased the IRF3 and NF-κB reporter activity when compared with the untreated cells ($p < 0.001$). However, the LPS-induced increases in IRF3 reporter activity were significantly decreased in the cells pretreated with AI or 6-OAAI. We also observed that 6-OAAI inhibited IRF3 reporter activity more effectively than AI. NF-κB reporter activity was also decreased in the cells pretreated with AI or 6-OAAI. These results indicate that AI or 6-OAAI may suppress the production of NO, iNOS, and IFN-β and pro-inflammatory cytokines through the inhibition of IRF3 and NF-κB activation.

4. Discussion

In this study, we demonstrated the anti-inflammatory effects of AI and 6-OAAI isolated from *S. rebaudiana* in LPS-stimulated RAW264.7 macrophage cells. Furthermore, we showed that AI and 6-OAAI inhibited IRF3 and NF-κB activation and the subsequent induction of the pro-inflammatory mediators NO, iNOS, IFN-β, MCP-1, TNF-α, IL-6, and IL-1β.

NO is a free radical produced from L-arginine and plays an important role in physiological homeostasis, including the reduction of blood pressure and the inhibition of platelet aggregation. Overproduction of NO by iNOS contributes to inflammation and a variety of diseases by reacting with macrophage-derived superox-

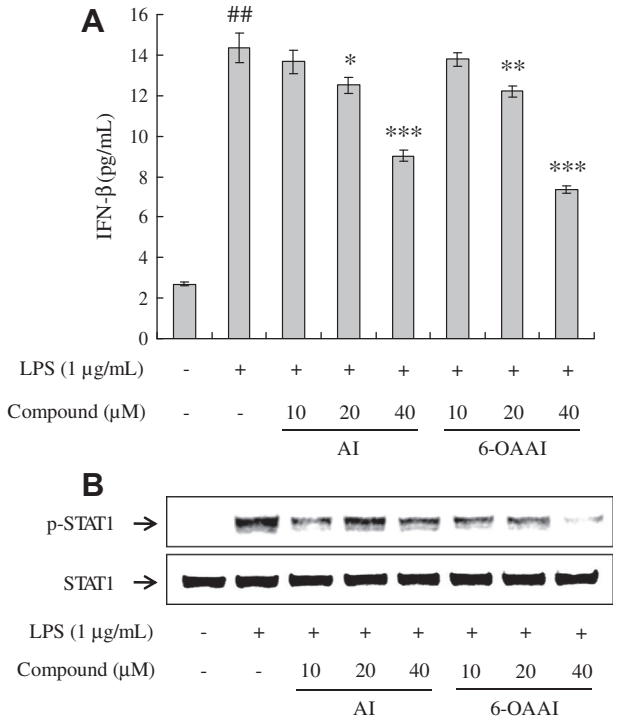

Fig. 4. Effect of AI and 6-OAAI on IFN-β expression (A) and STAT1 phosphorylation (B) in LPS-stimulated RAW264.7 macrophages. (A) RAW264.7 cells were treated with various concentrations of AI and 6-OAAI (10, 20, and 40 μM) for 1 h prior to the addition of LPS (1 μg/mL), and the cells were further incubated for 16 h. The IFN-β concentration in the culture supernatant was determined by ELISA. Error bars represent the mean ± SD. $^{\#\#}p < 0.001$ vs. control, $^{*}p < 0.05$ vs. LPS, $^{**}p < 0.01$ vs. LPS, $^{***}p < 0.001$ vs. LPS. (B) RAW264.7 cells were treated with various concentrations of AI and 6-OAAI (10, 20, and 40 μM) for 1 h prior to the addition of LPS (1 μg/mL) and the cells were further incubated for 4 h. The STAT1 phosphorylation levels were determined by western blotting.

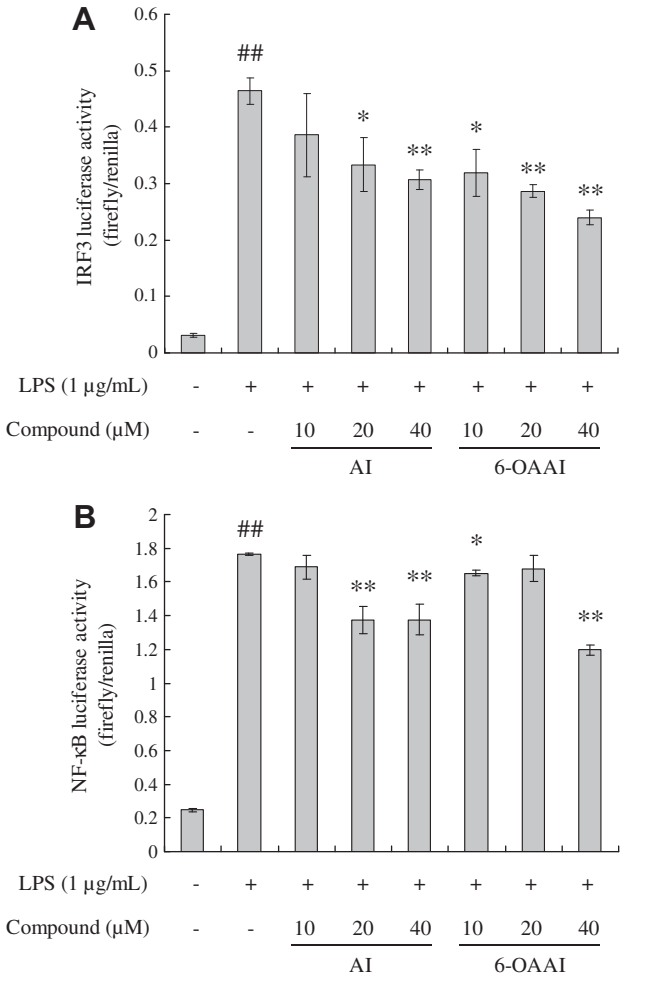

Fig. 5. Effect of AI and 6-OAAI on IRF3 (A) and NF-κB activation (B) in LPS-stimulated RAW264.7 macrophages. RAW264.7 cells were transiently transfected with pIRF3-luc and pNF-κB-luc reporter constructs. The pRL-TK vector was used as an internal control. These cells were treated with various concentrations of AI and 6-OAAI (10, 20, and 40 μM) for 1 h prior to the addition of LPS (1 μg/mL), and the cells were further incubated for 24 h. The levels of luciferase activities were determined. Error bars represent the mean ± SD. $^{\#\#}p < 0.001$ vs. control, $^{*}p < 0.05$ vs. LPS, $^{**}p < 0.01$ vs. LPS.

ide to produce highly cytotoxic peroxynitrite (Han et al., 2008). Several studies have reported that natural products from plants reduce LPS-induced NO production in RAW264.7 macrophage cells through the inhibition of iNOS expression (Bae et al., 2012; Byun, 2012). The results of the present study show that AI and 6-OAAI significantly inhibited the increase in NO and iNOS expression levels in LPS-stimulated RAW264.7 cells. These results demonstrate that AI and 6-OAAI suppress NO production by inhibiting iNOS expression levels.

LPS can induce pro-inflammatory cytokines and chemokines in inflammatory responses. Several studies have suggested that pro-inflammatory cytokines such as TNF-α, IL-6, and IL-1β induce the expression of iNOS, and thereby NO production, through the activation of NF-κB and MAPK (Kim et al., 2010; Maity et al., 2012). Arvelexin from *Brassica rapa* has been documented to suppress pro-inflammatory cytokines, such as TNF-α, IL-6, and IL-1β, that are secreted upon LPS stimulation in RAW264.7 cells (Shin et al., 2011). Moreover, Kou et al. (2011) have reported that arctigenin inhibits LPS-induced IL-6, IL-1β, and MCP-1 production in RAW264.7 cells. In agreement with previous reports, we showed that AI and 6-OAAI significantly inhibited the production of TNF-α, IL-6, IL-1β, and MCP-1 in LPS-stimulated RAW264.7 cells. These findings indicate that AI and 6-OAAI could suppress the inflammatory response via the inhibition of inflammatory cytokines.

LPS is known to generally activate two main branches of downstream signaling pathways: MyD88- and TRIF-dependent pathways in Toll-like receptor (TLR) signaling. Upon stimulation with LPS, NF-κB and MAPK are activated by the MyD88-dependent pathway, which results in inflammatory cytokine production (Kawai and Akira, 2006). Many studies have demonstrated that natural compounds suppress the inflammatory response by inhibiting the production of pro-inflammatory mediators via interfering with NF-κB and MAPK pathways (Shin et al., 2011; Yoon et al., 2010; Bharat Reddy and Reddanna, 2009). In the present study, the activation of NF-κB was markedly increased in LPS-stimulated RAW264.7 cells. However, AI or 6-OAAI treatment led to a significant decrease in the activation of NF-κB, suggesting that the anti-inflammatory activity of AI and 6-OAAI might be involved in the inhibition of NF-κB activation through the MyD88-dependent pathway. The exact mechanism of NF-κB activation by AI and 6-OAAI should be investigated in future studies.

In response to LPS stimulation, TRIF plays an important role in type I IFN induction, particularly of IFN-β. TRIF interacts with TANK-binding kinase-1 (TBK1), which mediates IRF3 activation, and in turn leads to induction of IFN-β. Through the proteins TRAF6 and RIP1, TRIF also activates NF-κB and MAPK, which is required for the induction of IFN-β (Kawai and Akira, 2006). IFN-β plays a critical role in the expression of iNOS via the activation of STAT1 in immune responses. A previous study reported that gold nanoparticles attenuate LPS-induced NO production through the inhibition of NF-κB and IFN-β/STAT1 pathways in RAW264.7 cells

(Ma et al., 2010). Therefore, we investigated whether AI or 6-OAAI inhibit the IFN-β/STAT1 pathway that is known to be activated by LPS-stimulation in RAW264.7 cells. Here, we found that AI and 6-OAAI significantly inhibited LPS-induced IFN-β production and STAT1 phosphorylation in RAW264.7 cells. We also showed that AI and 6-OAAI significantly decreased the activation of IRF3 and NF-κB in LPS-stimulated RAW264.7 cells. Park and Youn (2010) have shown that isoliquiritigenin suppresses IRF3 activation via the TRIF-dependent signaling pathway of TLR by targeting TBK1. Our results suggest that AI and 6-OAAI inhibit NO production and iNOS expression through the suppression of the IFN-β/STAT1 pathway by blocking the activation of IRF3 and NF-κB in LPS-stimulated RAW264.7 cells. Taken together, our results suggest that AI and 6-OAAI might modulate both MyD88- and TRIF-dependent pathways in TLR signaling. Therefore, characterization of the main target molecule and the upstream signaling pathway of AI and 6-OAAI needs to be further investigated.

The cell membrane contains both hydrophilic and hydrophobic compartments. The antioxidant action of a compound is known to be dependent not only on its structural antioxidant potential but also on its ability to pass through the plasma membrane (Pavlica and Gebhardt, 2010). Youdim et al. (2003) have reported that the permeation potential of flavonoids is consistent with the lipophilicity of the compounds. A recent study has demonstrated that the lipophilic diterpenes linearol and sidol with an acetyl group are more active than the hydrophilic diterpene foliol with a hydroxyl group (Gonzalez-Burgos et al., 2013). 6-OAAI differs structurally from AI in the fact that 6-OAAI has an acetyl group instead of the hydroxyl group that AI has. Our results indicate that 6-OAAI more effectively exhibited anti-inflammatory activity than AI, as measured by the inhibition of the production of pro-inflammatory mediators and the activation of transcription factors. We assume that 6-OAAI may have stronger effects than AI due to its higher lipophilicity, which is the ability of a chemical compound to pass through the cell membrane.

In summary, our results demonstrate that AI and 6-OAAI inhibited the production of NO, iNOS, and pro-inflammatory cytokines (TNF-α, IL-6, IL-1β, and MCP-1) in LPS-stimulated RAW264.7 macrophages. Moreover, AI and 6-OAAI suppressed the phosphorylation of STAT1 and the production of IFN-β in LPS-stimulated RAW264.7 macrophages. Furthermore, AI and 6-OAAI treatment inhibited the activation of IRF3 and NF-κB in LPS-stimulated RAW264.7 macrophages. Therefore, we suggest that AI and 6-OAAI should be considered as candidate potential anti-inflammatory agents for the treatment of inflammatory diseases. Further studies are required to elucidate the specific mechanisms and clinical therapeutic potential of AI and 6-OAAI.

Conflict of Interest

The authors declare that there are no conflicts of interest.

Acknowledgement

This research was supported by the Ministry of Education, Science and Technology (MEST), Republic of Korea.

Appendix A. Supplementary material

Supplementary data associated with this article can be found, in the online version, at http://dx.doi.org/10.1016/j.fct.2013.09.011.

References

Bae, D.S., Kim, Y.H., Pan, C.H., Nho, C.W., Samdan, J., Yansan, J., Lee, J.K., 2012. Protopine reduces the inflammatory activity of lipopolysaccharide-stimulated murine macrophages. BMB Rep. 45, 108–113.
Bharat Reddy, D., Reddanna, P., 2009. Chebulagic acid (CA) attenuates LPS-induced inflammation by suppressing NF-κB and MAPK activation in RAW 264.7 macrophages. Biochem. Biophys. Res. Commun. 381, 112–117.
Byun, M.W., 2012. Anti-inflammatory activity of austroinulin from *Stevia rebaudiana* in LPS-induced RAW264.7 cells. J. Korean Soc. Food Sci. Nutr. 41, 456–461.
Chan, P., Tomlinson, B., Chen, Y.J., Liu, J.C., Hsieh, M.H., Cheng, J.T., 2000. A double-blind placebo-controlled study of the effectiveness and tolerability of oral stevioside in human hypertension. Br. J. Clin. Pharmacol. 50, 215–220.
Dacome, A.S., da Silva, C.C., da Costa, C.E.M., Fontana, J.D., Adelmann, J., da Costa, S.C., 2005. Sweet diterpenic glycoside balance of a new cultivar of *Stevia rebaudiana* (Bert.) Bertoni: isolation and quantitative distribution by chromatographic, spectroscopic, and electrophoretic methods. Process Biochem. 40, 3587–3594.
Ferrero-Miliani, L., Nielsen, O.H., Andersen, P.S., Girardin, S.E., 2006. Chronic inflammation: importance of NOD2 and NALP3 in interleukin-1β generation. Clin. Exp. Immunol. 147, 227–235.
Gonzalez-Burgos, E., Carretero, M.E., Gomez-Serranillos, M.P., 2013. Involvement of Nrf2 signaling pathway in the neuroprotective activity of natural kaurane diterpenes. Neuroscience 231, 400–412.
Han, J.M., Lee, W.S., Kim, J.R., Son, J., Kwon, O.H., Lee, H.J., Lee, J.J., Jeong, T.S., 2008. Effect of 5-O-methylhirsutanonol on nuclear factor-κB-dependent production of NO and expression of iNOS in lipopolysaccharide-induced RAW264.7 cells. J. Agric. Food Chem. 56, 92–98.
Heo, S.J., Yoon, W.J., Kim, K.N., Ahn, G.N., Kang, S.M., Kang, D.H., Affan, A., Oh, C., Jung, W.K., Jeon, Y.J., 2010. Evaluation of anti-inflammatory effect of fucoxanthin isolated from brown algae in lipopolysaccharide-stimulated RAW 264.7 macrophages. Food Chem. Toxicol. 48, 2045–2051.
Jeppesen, P.B., Gregersen, S., Alstrup, K.K., Hermansen, K., 2002. Stevioside induces antihyperglycaemic, insulinotropic and glucagonostatic effects in vivo: studies in the diabetic Goto-Kakizaki (GK) rats. Phytomedicine 9, 9–14.
Kawai, T., Akira, S., 2006. TLR signaling. Cell Death Differ. 13, 816–825.
Kim, K.N., Heo, S.J., Yoon, W.J., Kang, S.M., Ahn, G., Yi, T.H., Jeon, Y.J., 2010. Fucoxanthin inhibits the inflammatory response by suppressing the activation of NF-κB and MAPKs in lipopolysaccharide-induced RAW 264.7 macrophages. Eur. J. Pharmacol. 649, 369–375.
Kou, X., Qi, S., Dai, W., Luo, L., Yin, Z., 2011. Arctigenin inhibits lipopolysaccharide-induced iNOS expression in RAW264.7 cells through suppressing JAK–STAT signal pathway. Int. Immunopharmacol. 11, 1095–1102.
KrÖche, K.D., Fensel, K., Kolb-bachofen, V., 1998. Inducible nitric oxide synthase in human diseases. Clin. Exp. Immunol. 113, 147–156.
Lee, K.G., Shibamoto, T., 2001. Inhibition of malonaldehyde formation from blood plasma oxidation by aroma extracts and aroma components isolated from clove and eucalyptus. Food Chem. Toxicol. 39, 1199–1204.
Lemus-Mondaca, R., Vega-Galvez, A., Zura-Bravo, L., Ah-Hen, K., 2012. *Stevia rebaudiana* Bertoni, source of a high-potency natural sweetener: a comprehensive review on the biochemical, nutritional and functional aspects. Food Chem. 132, 1121–1132.
Lu, Y., Suh, S.J., Kwak, C.H., Kwon, K.M., Seo, C.S., Li, Y., Jin, Y., Li, X., Hwang, S.L., Kwon, O., Chang, Y.C., Park, Y.G., Park, S.S., Son, J.K., Kim, C.H., Chang, H.W., 2012. Saucerneol F, a new lignan, inhibits iNOS expression via MAPKs, NF-κB and AP-1 inactivation in LPS-induced RAW264.7 cells. Int. Immumopharmacol. 12, 175–181.
Ma, J.S., Kim, W.J., Kim, J.J., Kim, T.J., Ye, S.K., Song, M.D., Kang, H., Kim, D.W., Moon, W.K., Lee, K.H., 2010. Gold nanoparticles attenuate LPS-induced NO production through the inhibition of NF-κB and IFN-β/STAT1 pathways in RAW264.7 cells. Nitric Oxide-Biol. Chem. 23, 214–219.
Maity, B., Yadav, S.K., Patro, B.S., Tyagi, M., Bandyopadhyay, S.K., Chattopadhyay, S., 2012. Molecular mechanism of the anti-inflammatory activity of a natural diarylnonanoid, malabaricone C. Free Radic. Biol. Med. 52, 1680–1691.
Mordan, L.J., Burnett, T.S., Zhang, L.X., Tom, J., Cooney, R.V., 1993. Inhibitors of endogenous nitrogen oxide formation block the promotion of neoplastic transformation in C3H10T1/2 fibroblasts. Carcinogenesis 14, 1555–1559.
Muanda, F.N., Soulimani, R., Diop, B., Dicko, A., 2011. Study on chemical composition and biological activities of essential oil and extracts from *Stevia rebaudiana* Bertoni leaves. LWT-Food Sci. Technol. 44, 1865–1872.
Ohshima, H., Bartsch, H., 1994. Chronic infections and inflammatory processes as cancer risk factors: possible role of nitric oxide in carcinogenesis. Mutat. Res. 305, 253–264.
Oshima, Y., Saito, J., Hikino, H., 1986. Sterebins A, B, C and D, bisnorditerpenoids of *Stevia rebaudiana* leaves. Tetrahedron 42, 6443–6446.
Oshima, Y., Saito, J., Hikino, H., 1988. Sterebins E, F, G and H, diterpenoids of *Stevia rebaudiana* leaves. Phyochemistry 27, 624–626.
Park, S.J., Youn, H.S., 2010. Isoliquiritigenin suppresses the Toll-interleukin-1 receptor domain-containing adapter inducing interferon-β (TRIF)-dependent signaling pathway of Toll-like receptors by targeting TBK1. J. Agric. Food Chem. 58, 4701–4705.
Pavlica, S., Gebhardt, R., 2010. Protective effects of flavonoids and two metabolites against oxidative stress in neuronal PC12 cells. Life Sci. 86, 79–86.

Porto, T.S., Rangel, R., Furtado, N.A.J.C., de Carvalho, T.C., Martins, C.H.G., Veneziani, R.C.S., Da Costa, F.B., Vinholis, A.H.C., Cunha, W.R., Heleno, V.C.G., Ambrosio, S.R., 2009. Pimarane-type diterpenes: antimicrobial activity against oral pathogens. Molecules 14, 191–199.

Quijano, L., Calderon, J.S., Gomez, F., Vega, J.L., Rios, T., 1982. Diterpenes from *Stevia monardaefolia*. Phytochemistry 21, 1369–1371.

Shin, J.S., Noh, Y.S., Lee, Y.S., Cho, Y.W., Baek, N.I., Choi, M.S., Jeong, T.S., Kang, E., Chung, H.G., Lee, K.T., 2011. Arvelexin from *Brassica rapa* suppresses NF-κB-regulated pro-inflammatory gene expression by inhibiting activation of IκB kinase. Br. J. Pharmacol. 164, 145–158.

Sholichin, M., Yamasaki, K., Miyama, R., Yahara, S., Tanaka, O., 1980. Labdane-type diterpenes from *Stevia rebaudiana*. Phytochemistry 19, 326–327.

Shukla, S., Mehta, A., Bajpai, V.K., Shukla, S., 2009. *In vitro* antioxidant activity and total phenolic content of ethanolic leaf extract of *Stevia rebaudiana* Bert. Food Chem. Toxicol. 47, 2338–2343.

Vallim, M.A., Barbosa, J.E., Cavalcanti, D.N., De-Paula, J.C., da Silva, V.A.G.G., Teixeira, V.L., de Palmer Paixao, I.C.N., 2010. *In vitro* antiviral activity of diterpenes isolated from the Brazilian brown alga *Canistrocarpus cervicornis*. J. Med. Plants Res. 4, 2379–2382.

Wang, S.Y., Wu, J.H., Shyur, L.F., Kuo, Y.H., Chang, S.T., 2002. Antioxidant activity of abietane-type diterpenes from heartwood of *Taiwania cryptomerioides* Hayata. Holzforschung 56, 487–492.

Yoon, W.J., Moon, J.Y., Song, G., Lee, Y.K., Han, M.S., Lee, J.S., Ihm, B.S., Lee, W.J., Lee, N.H., Hyun, C.G., 2010. *Artemisia fukudo* essential oil attenuates LPS-induced inflammation by suppressing NF-κB and MAPK activation in RAW 264.7 macrophages. Food Chem. Toxicol. 48, 1222–1229.

Youdim, K.A., Dobbie, M.S., Kuhnle, G., Proteggente, A.R., Abbott, N.J., Rice-Evans, C., 2003. Interaction between flavonoids and the blood-brain barrier: in vitro studies. J. Neurochem. 85, 180–192.